Adaptive laboratory evolution of Rhodosporidium toruloides to inhibitors derived from lignocellulosic biomass and genetic variations behind evolution

Liu, Zhijia; Radi, Mohammad; Mohamed, Elsayed T. T.; Feist, Adam M.; Dragone, Giuliano; Mussatto, Solange I.

Published in:
Bioresource Technology

Link to article, DOI:
10.1016/j.biortech.2021.125171

Publication date:
2021

Document Version
Peer reviewed version

Journal Pre-proofs

Adaptive laboratory evolution of *Rhodosporidium toruloides* to inhibitors derived from lignocellulosic biomass and genetic variations behind evolution

Zhijia Liu, Mohammad Radi, Elsayed T.T. Mohamed, Adam M. Feist, Giuliano Dragone, Solange I. Mussatto

PII: S0960-8524(21)00510-1
DOI: https://doi.org/10.1016/j.biortech.2021.125171
Reference: BITE 125171

To appear in: *Bioresource Technology*

Received Date: 8 March 2021
Revised Date: 7 April 2021
Accepted Date: 8 April 2021

Please cite this article as: Liu, Z., Radi, M., Mohamed, E.T.T., Feist, A.M., Dragone, G., Mussatto, S.I., Adaptive laboratory evolution of *Rhodosporidium toruloides* to inhibitors derived from lignocellulosic biomass and genetic variations behind evolution, *Bioresource Technology* (2021), doi: https://doi.org/10.1016/j.biortech.2021.125171

Adaptive laboratory evolution of *Rhodosporidium toruloides* to inhibitors derived from lignocellulosic biomass and genetic variations behind evolution

Zhijia Liu [a], Mohammad Radi [a], Elsayed T. T. Mohamed [a], Adam M. Feist [a,b], Giuliano Dragone [c], Solange I. Mussatto [c,*]

[a] *Novo Nordisk Foundation Center for Biosustainability, Technical University of Denmark, Kemitorvet, Building 220, 2800, Kongens Lyngby, Denmark*

[b] *Department of Bioengineering, University of California, San Diego, 9500 Gilman Drive, La Jolla, CA 92093-0412, USA*

[c] *Department of Biotechnology and Biomedicine, Technical University of Denmark, SøltoftsPlads, Building 223, 2800, Kongens Lyngby, Denmark*

[*] Corresponding author.

E-mail address: smussatto@dtu.dk; solangemussatto@hotmail.com (S.I. Mussatto)

ABSTRACT

Using lignocellulosic biomass hydrolysate for the production of microbial lipids and carotenoids is still a challenge due to the poor tolerance of oleaginous yeasts to the inhibitors generated during biomass pretreatment. In this study, a strategy of adaptive laboratory evolution in hydrolysate-based medium was developed to improve the tolerance of *Rhodosporidium toruloides* to inhibitors present in biomass hydrolysate. The evolved strains presented better performance to grow in hydrolysate medium, with a significant reduction in their lag phases, and improved ability to accumulate lipids and produce carotenoids when compared to the wild-type starting strain. In the best cases, the lag phase was reduced by 72 h and resulted in lipid accumulation of 27.89±0.80% (dry cell weight) and carotenoid production of 14.09±0.12 mg/g (dry cell weight). Whole genome sequencing analysis indicated that the wild-type strain naturally contained tolerance-related genes, which provided a background that allowed the strain to evolve in biomass-derived inhibitors.

Keywords: Adaptive laboratory evolution; Tolerance; Inhibitors; Hydrolysate; *Rhodosporidium toruloides*

1. Introduction

In the last years, oleaginous yeasts have attracted increased attention due to their ability to produce lipids and carotenoids from different carbon sources. In addition, the accumulation of lipids in oleaginous yeasts can reach 70% of their dry cell weight under nutrient starvation conditions (Probst et al., 2016). Lipids produced by oleaginous yeasts mainly include palmitic acid (C16:0), oleic acid (C18:1) and linoleic acid (C18:2), which have a composition similar to cocoa butter and palm oil, being good alternatives to replace plant oils to produce fatty acid esters based chemicals such as soaps, cleansers and personal care products (Vasconcelos et al., 2019; Liu et al., 2020a). In addition, fatty acids produced by oleaginous yeasts can be used for biodiesel production, since the cetane number and clod filter plugging points of methyl esters of those fatty acids, which are important parameters to evaluate the quality of biodiesel, are in the range of EU standards (Bonturi et al., 2015; Ramos et al., 2009).

Besides lipids, some oleaginous yeasts can also produce carotenoids, among of which, β-carotene, γ-carotene, torulene and torularhodin are the most common (Chandi and Gill, 2011). Carotenoids present anti-oxidant and anti-tumor activities, and help reduce the risk of many diseases (Novoveská et al., 2019). Therefore, these compounds have been widely utilized in food, feed, pharmaceutical and cosmetic industries, and their market is estimated to reach $2.00 billion by 2026 (MarketsandMarkets, 2020). At present, edible plants are the main sources of carotenoids. Using oleaginous yeasts to replace edible plants to produce lipids and carotenoids can help reduce the conflict with food production. Then, seeking for cheap and renewable carbon sources for cultivation of oleaginous yeast is a key strategy to reach this sustainable goal.

Previous studies have demonstrated that agricultural and agro-industrial residues, wastewaters, and crude glycerol can be used as carbon sources for oleaginous yeast cultivation (Arous et al., 2016; Kitcha and Cheirsilp, 2013; Liu et al., 2020). Among them, lignocellulosic biomass is highly attractive because it is non-edible, has a low cost and is abundant around the world. To be used in fermentation processes, a pretreatment step is required to recover sugars from biomass structure. However, besides sugars, other compounds, which are toxic to microorganisms, are also released from the material's structure or formed during their partial degradation. Such toxic/inhibitory compounds are divided into 3 main groups: furan aldehydes, aliphatic acids, and phenolic compounds. Furan aldehydes, such as furfural and hydroxymethylfurfural (HMF), result from the degradation of pentose and hexose sugars, respectively. The further degradation of HMF lead to the formation of formic acid and levulinic acids, which are aliphatic acids. Phenolic compounds including vanillic acid, syringic acid, 4-hydroxybenzaldehyde, *p*-coumaric acid, vanillin and syringaldehyde, among others, are obtained from lignin degradation (Mussatto and Roberto, 2004). The presence of these inhibitory compounds in biomass hydrolysate can significantly influence the growth and product accumulation in oleaginous yeast (Liu et al., 2020).

Although different methods have been proposed to reduce the concentration of inhibitors in biomass hydrolysate in order to improve the microbial performance during fermentation, detoxification methods result in additional costs to the overall process (Mussatto and Dragone, 2016). Other strategies that can be used to improve the tolerance of oleaginous yeasts to inhibitors derived from lignocellulosic biomass include adaptive laboratory evolution (ALE) and genetic engineering. When compared with random engineering, ALE is easier to perform and mutant strains with desired

characters can be obtained by cultivating generations of strains under selective pressure conditions. In the sequence, whole genome sequencing analysis can help to unravel the mutation mechanism and provide knowledge for genetic engineering.

So far, the use of the ALE technique in hydrolysate-based medium has been little explored to improve the performance of oil producing microorganisms. In the present study, an ALE strategy was designed to improve the tolerance of the oleaginous yeast *Rhodosporidium toruloides* NRRL Y-1091 toward inhibitors derived from biomass pretreatment. The growth profile, lipid and carotenoid production of wild-type and evolved strains were then compared. Finally, a whole genome sequencing analysis of wild-type and evolved strains was performed to explain the mutation mechanism and genetic variations behind evolution.

2. Materials and methods

2.1 Microorganism and cultivation conditions

The wild-type oleaginous yeast *Rhodosporidium toruloides* NRRL Y-1091 was used in this study. The strain was obtained from the Agricultural Research Culture Collection, USA and stored at -80 ℃ in 20% glycerol. In the pre-cultivation step, one loop of yeast cells was transferred to 100 mL YPD medium in 250 mL flasks and cultivated at 30 ℃, 250 rpm for 72 h. To obtain single colonies, the YPD broth was diluted 20.000-folds with autoclaved distilled water. After that, 100 µL of diluted YPD broth was spread on YPD agar plates and incubated at 30 ℃ for 5 days.

2.2 Preparation of wheat straw hydrolysate

Wheat straw was provided by the Danish Technological Institute (Denmark). The material was milled to a size of about 180-1800 mm and then submitted to hydrothermal pretreatment and enzymatic hydrolysis in order to produce a sugar-rich hydrolysate, which was also decolorized to be used in the ALE experiments. The conditions used to produce the hydrolysate were previously described (Liu et al., 2020). **Table 1** summarizes the composition of the hydrolysates (decolorized and non-decolorized) used for the ALE experiments.

The concentrations of glucose, xylose and acetic acid in the hydrolysate was quantified using a HPLC system (Dionex Ultimate 3000, Germany) equipped with an Aminex HPX-87H column (300 × 7.8 mm, Bio-Rad, USA) eluted with 0.005 M H_2SO_4 at 50 ℃ for 50 min with a flow rate of 0.6 mL/min. The concentrations of furfural, HMF, levulinic acid, vanillic acid, syringic acid, 4-hydroxybenzaldehyde, *p*-coumaric acid, vanillin and syringaldehyde were measured by using the same HPLC system, but equipped with a UV detector at 280 nm and a Zorbax eclipse plus C18 column (Agilent, USA) eluted with mobile phases composed by A: 0.05% (v/v) acetic acid in water and B: acetonitrile at a flow rate of 1 mL/min. The gradient elution started with 5% of B and linearly increased to 60% over 5 min and further increased to 90% of B over 0.5 min. This gradient was kept at this ratio for 2 min and returned to 5% of B until 10 min. Total phenolic compounds were determined by a colorimetric method (Ballesteros et al., 2014). All the standards used for analysis were purchased from Sigma-Aldrich.

2.3 Adaptive laboratory evolution (ALE)

The ALE experiment was performed in an automated liquid handling robot platform in which the strains were incubated in 15-mL plastic tubes with caps in a heat

145 block kept at 30 ℃ and aerated by magnetic stirring at 1200 rpm. The growth of the
146 strains was monitored by absorbance reading at 600 nm using a Teach Sunrise
147 microplate reader (Tecan, Männedorf, Switzerland) connected to the automated
148 platform. Continuous cultivations of 10 replicates of the wild-type strain were
149 performed in medium containing increasing concentration of wheat straw hydrolysate.
150 To obtain different concentration of inhibitors for the experiments, the hydrolysate was
151 diluted with synthetic medium composed by the same amount of sugars, supplemented
152 with 1.79 g/L yeast nitrogen base without amino acid and ammonium sulfate (Sigma-
153 Aldrich) and 1 g/L NH_4Cl, pH 4.9.

154 The driving force for the ALE experiments was based on increasing the
155 concentration of inhibitor gradually and making the mutant strains enrich in population.
156 The whole evolution process was divided in two rounds. In the first round, the
157 decolorized hydrolysate was used and a screening of the wild-type strain in 25%, 50%,
158 75% and 100% hydrolysate was performed to decide the starting point of the evolution.
159 When the growth rate of the strains in certain level of the decolorized hydrolysate
160 increased compared to the growth rate observed in the screening experiment, then 10%
161 of the culture was transferred to a higher concentration of decolorized hydrolysate. This
162 process was repeated until all replicates of the strains were able to grow well in 100%
163 decolorized hydrolysate. Then, the ALE strategy was repeated using non-decolorized
164 hydrolysate until the strains could grow well in 100% hydrolysate.

165

166 *2.4 Comparison of wild-type and evolved strains*

167 The evolved and wild-type strains were cultivated in the synthetic medium
168 described above in shaking flasks at 30 ℃, 250 rpm for 72h. Afterward, cells were

collected by centrifugation (5000 rpm, 5 min), washed with sterilized distilled water and suspended in non-decolorized wheat straw hydrolysate supplemented with 1 g/L NH_4Cl to obtain a cell concentration of 1 g/L. The cell mass was estimated using a calibration curve between absorbance of cells in distilled water at 600 nm and dry weight of cells.

The assays for comparison of the wild-type and evolved strains were then performed in 24 deep well plates with 3 mL working volume in each well. Every 24 h, 2 well samples per strain were taken to measure the cell mass and °Brix (total soluble solids in aqueous solution). Lipid and carotenoid contents were determined at the end of the cultivation (120/144 h).

2.5 Analysis of lipids and carotenoids produced by wild-type and evolved strains

For the cell disruption step, cells from 2 mL fermentation broth were collected by centrifugation (5000 rpm, 5 min), washed twice with distilled water, then suspended in 1 mL distilled water and transferred to a lysing matrix E tube (6914-500, MP Biomedicals, France). The lysing tubes were beaten on a bead beater (Precellys 24, Bertin Technologies, France) for 3 cycles of 60 s at 5000 rpm, with 60 s break after each cycle. After that, all cell debris, beads and liquid in the beating tubes were transferred into new glass tubes with screw caps.

For total lipid quantification, the disrupted cells were extracted 3 times with a solution of chloroform:methanol (1:1.25). After 3500 rpm, 5 min centrifugation, the bottom phase was withdrawn and dried under N_2 atmosphere for total lipid analysis. Before gas chromatograph analysis, the fatty acids were methylated. The methylation and analysis were conducted according to the method described by Breuer et al. (2013)

on a gas chromatograph system (Agilent 7890, USA) equipped with a Supelco Nucol™ 25357 (30 m × 530 µm × 1.0 µm) column.

For carotenoid quantification, 2 mL of chloroform were added to each tube containing the disrupted cells and the mixture was vortexed for 10 min. Then the tubes were centrifuged at 3500 rpm for 5 min and the bottom phase was taken into another clean glass tube. The extraction was repeated 3 times and the combined chloroform fractions were dried under N_2 flow. The extracted carotenoids were redissolved in 2 mL acetone containing 0.2% (w/v) BHT (butylated hydroxytoluene) and inserted in a brown HPLC glass vial for further analysis. A Shimadzu Nexera UHPLC system equipped with a D2&W 190-800 nm PDA detector and a C30 reversed-phase carotenoid column (3 µm, 250 × 4.6 mm - YMC, Japan) was used for carotenoid quantification. The HPLC conditions for carotenoid detection were adapted from the method described by Søltoft et al. (2011). The carotenoid standards β-carotene and γ-carotene (Sigma-Aldrich) were detected at their maximum absorbance wavelength (450 and 461 nm, respectively). Torulene was quantified using γ-carotene as standard (Liu et al., 2021).

2.6 Whole genome sequencing

To identify the common mutations and important genes responsible for the mutations, the whole genome of the 7 best evolved strains (identified as CH1, CH3, CH4, CH5, CH6, CH8, CH10) were sequenced, and then compared with the genome sequence of the wild-type starting stain. Single colonies of all these 8 strains were picked up from YPD agar plates and cultivated in synthetic medium at 30°C, 250 rpm for 72h. The DNA of the strains was extracted using a Quick-DNA™ fungal/bacterial miniprep kit (Zymo Research, USA). To prepare the reference genome, the DNA of the

wild-type strain was sequenced by the PacBio RS platform (10-kb SMRT library) and Illumina HiSeq 2000 platform at 2x150 paired-end reads. The genome of the evolved strains was sequenced by the same Illumina platform at 2x150 paired-end reads.

2.7 *De novo* assembly and function annotation

After removing low quality reads, the clean data was corrected using the softwares Pbdagcon and Falcon Consensus. The corrected reads were assembled using softwares such as Celera Assembler, Falcon and SMRT Analysis. Then, the best assembly result was chosen and the single reads of it was corrected with Illumina Hiseq data using GATK software. The gap between contig and scaffold was filled with long inset size paired-end reads using SSPACE Basic. To determine the location of the genes, the homology prediction was conducted with Gene Wise. Then, *de novo* prediction tools including SNAP, Augustus, Gene Markers were used to predict the gene models. Non-coding RNA was identified by RNAmmer and tRNAscan software. The transposon sequence was found by aligning the assembly with the known transposon sequence database (RepeatMasker, RepeatProteinMasker, buildXDFDatabase). Gene function annotation was completed by blasting genes with different databases including P450, VFDB, ARDB, TF, CAZY, KINASE, SWISSPROT, NOG, COG, CARD, CWDE, NR, KEYWORD, DBCAN, TCDB, T3SS, TREMBL, IPR, PHI, KEGG, GO, PHOSPHATASE, KOG databases.

2.8 Mutation detection

After removing low quality reads, the clean data of the evolved strains was mapped to the reference using the BWA software. The Picard tool was used to filter repeat reads.

The single nucleotide polymorphisms (SNPs) and insertion and deletion of bases into genome (InDels) of evolved strains were detected by the GATK software and compared with the reference strain.

2.9 Statistical analysis

Significant differences among samples were verified by analysis of variance at a significance level of 0.05, using the software OriginPro 2018b (OriginLab, USA).

3. Results and discussion

3.1 ALE strategy and fitness changes of strains during evolution

Biomass hydrolysates usually contain a mixture of different inhibitory compounds and their synergistic effect may strongly affect the microbial performance during fermentation (Mussatto and Roberto, 2004). Therefore, the ALE strategy used in the present study consisted in using biomass hydrolysate as culture medium for evolution in order to improve the ability of the strain to grow in the presence of different compounds present simultaneously in the medium. To improve the tolerance of *R. toruloides* to the inhibitory compounds, two rounds of ALE were performed: a first-round, where the yeast was evolved in decolorized hydrolysate, and a second-round, where the previously evolved yeast was now evolved in non-decolorized (raw) hydrolysate. It is worth highlighting that, although the decolorization step partially removed some inhibitors from the hydrolysate, the decolorization removed mainly compounds contributing to the color of the medium, and a significant amount of inhibitors was still present in the hydrolysate after this step (**Table 1**).

To boost the tolerance of the strain to the toxic compounds, the level of toxicity to be applied must be in an appropriate range since a very low concentration of inhibitors may not be enough to promote selective pressure for the strain to evolve, while a very high concentration of inhibitors may cease the growth of the strain. Therefore, before the ALE experiments, a screening step was performed by cultivating the yeast in different concentrations of decolorized hydrolysate. It was observed in these experiments that the growth rate of the yeast cultivated in 25% decolorized hydrolysate was comparable to that observed in synthetic medium (0.27 h^{-1}). So, 25% of decolorized hydrolysate was used as starting concentration for ALE. The concentration of the hydrolysate was increased when the growth rate of the strains reached approx. 0.15 h^{-1}. After 21 days of ALE, all replicates were able to grow in 100% decolorized hydrolysate (**Table 2**) and their growth rates were similar to that observed in synthetic medium.

Before starting the second-round of ALE in non-detoxified hydrolysate, another growth screening was conducted, and it was observed that, except CH1, CH2, CH3 and CH4, the other replicates were already able to grow in 80% non-decolorized hydrolysate. Therefore, the starting concentration of hydrolysate for the second-round ALE for these 6 populations was 80%. For the other 4 populations, the starting concentration of hydrolysate was adjusted to 30%, 70%, 10% and 70% for CH1, CH2, CH3 and CH4, respectively. After 41 days of ALE, most of the strains were able to grow in100% non-decolorized hydrolysate (**Table 2**). Confirmation tests revealed that, except the strains CH1 and CH3, all the other evolved strains were able to grow in 100% hydrolysate with fitness similar to that observed in synthetic medium.

These results allow concluding that the ALE strategy was successfully applied to improve the tolerance of the oleaginous yeast to biomass inhibitors. In future studies,

analysis of the cell viability measurement by colony forming units (CFU) could also be introduced to further refine the ALE monitoring, giving indications on the number of living cells during the evolution process. This can be especially relevant in media where color can affect the OD measurement, which was not the case of the present study.

3.2 Comparison of growth profile of wild-type and evolved strains in non-decolorized hydrolysate

Fig. 1 shows the growth profile of the wild-type starting strain and all the 10 evolved strains cultivated in non-decolorized hydrolysate. As can be seen, all the evolved strains (except CH3) presented shorter lag phase when compared to the wild-type strain (**Fig. 1A**). Among them, CH6 and CH10 started to grow after 24 h only, while CH2, CH4, CH5, CH7 and CH8 started to grow after 48h. The lag phase for CH9 lasted 72 h, while the CH3 and the wild-type strains started to grow after 96 h. However, it was found that sugars in the hydrolysate were not totally consumed for any of the strains during the 120 h of cultivation (data not shown), and the cell mass accumulated was also relatively low for all the strains. The low sugars consumption and cell mass accumulation could be an indication that the nitrogen source in wheat straw hydrolysate was not high enough to favor the yeast propagation. Therefore, in a second step, the strains were cultivated in hydrolysate supplemented with 1 g/L NH_4Cl. After nitrogen supplementation (**Fig. 1B**), sugars consumption and cell mass accumulation of wild-type and evolved strains were improved. However, similar as before, the wild-type strain entered in the exponential phase after 96 h, while the evolved strains had a shorter lag phase. When observing the strains, the performance of CH6 was relatively consistent in both media (supplemented or not with nitrogen) with a lag phase of only

312 24 h and more cell mass accumulated than the other strains in both cases. Such result
313 indicates that the hydrolysate supplementation with nitrogen had a more pronounced
314 effect on the cell mass accumulation than in the lag phase.
315
316 *3.3 Comparison of lipid and carotenoid accumulation for the wild-type and evolved*
317 *strains*
318 After the evolution, the ability of the wild-type and evolved strains to accumulate
319 lipids and carotenoids was also evaluated and compared. Quantifications were
320 performed after 144 h of fermentation using non-decolorized hydrolysate supplemented
321 with nitrogen (1 g/L NH_4Cl). As can be seen in **Fig. 2**, significant differences ($p<0.05$)
322 in terms of product accumulation were observed for the wild-type and evolved strains.
323 Except CH2, all the evolved strains were able to accumulate more lipids than the
324 parental strain. CH4 was the best lipid producer, accumulating 27.89±0.80% of the cell
325 weight in lipids. To better understand the effect of the evolution on lipid production by
326 the yeast, the composition of fatty acids produced by the wild-type and evolved strains
327 was also determined and compared. As shown in **Table 3**, palmitic acid (C16:0) and
328 oleic acid (C18:1) were the main fatty acids produced by all the strains. This result
329 reveals that although the ability of the strain to accumulate lipids was improved after
330 ALE, the evolution did not change the lipid synthesis pathway of the yeast.
331 Carotenoids were also accumulated in significantly higher amount ($p<0.05$) in the
332 evolved strains than in the wild-type (**Fig 2A**). The best carotenoid producers were CH2
333 and CH7, which accumulated 13.89±0.09 mg/g and 14.09±0.12 mg/g of cell weight in
334 carotenoids, respectively (the carotenoid accumulation by these two strains was similar
335 at $p<0.05$). All the strains produced β-carotene, γ-carotene and torulene; with γ-carotene

and torulene being the carotenoids produced in higher amount (**Table 4**). So, similarly to what was observed for lipids, the ability of the strain to accumulate carotenoids was improved after ALE, but the evolution did not change the profile of the carotenoids produced by the yeast. The difference observed on the production of carotenoids by the evolved strains was also reflected on the color of the cells at the end of the cultivation, which was darker for the evolved strains.

In oleaginous yeasts, carotenoids are located in the fat rich region in yeast cells, and play a protective role of resistance to light and oxidation damages from the cultivation environment (Avalos and Carmen Limón, 2015). To improve the production of carotenoids, radiation or oxidation conditions can be used during the ALE process, for example (Reyes et al., 2014). In the present study, ALE of *R. toruloides* was performed in wheat straw hydrolysate (which contains a mixture of inhibitory compounds) and also resulted in an improved production of carotenoids. Such improvement could be the response of the yeast to oxidation stress. Phenolic compounds present in the hydrolysates can enhance the generation of reactive oxygen species including H_2O_2, O_2^- and OH^-, which cause enzyme denaturation, cytoskeleton damages and cell death (Wang et al., 2018; Ibraheem and Ndimba, 2013). Furfural, which is another inhibitor usually found in hydrolysates, may also cause oxidation damages to yeast (Allen et al., 2010).

3.4 Genome sequencing and annotation for the wild-type strain

The combination of Illumina HiSeq and PacBio RS sequencing and *de novo* assembly of the wild-type *R. toruloides* yielded a 21.5 Mb genome with an average 101× coverage. This genome was composed of 263 contigs and 68 scaffolds, in which

8387 coding genes and 236 ncRNA were distributed. Regarding to the annotation results, 98.85% of genes could be mapped to definitive functions via blasting against CAZy, Kinase, Swissprot, NOG, KEGG, KOG, Tremble, GO, T3SS and others total 23 databases.

The sequencing analysis revealed that the wild-type strain naturally contains tolerance-related genes, which provided a background that allowed the strain to evolve in biomass-derived inhibitors. From the annotation result, 25 alcohol dehydrogenases encoding genes, 18 aldehyde reductases encoding genes, and 4 alcohol oxidases were found in this yeast, which is in agreement with the study of Wang et al. (2016). Other functional genes, such as stress response genes and other tolerance related genes were also identified.

3.5 Mutations detected in evolved strains

In this step of the study, the genome of the 7 best performing evolved strains were aligned to the reference genome of the wild-type starting strain with the aim of identifying the mutations resulting from the ALE process. Mutation types and numbers in each evolved strain were summarized in **Fig.3.** Missense nonsynonymous SNPs was the mutation that most often occurred, being observed around 2500 times in each evolved strain. This mutation can change the amino acid sequence of protein. Similarly, insertions and deletions occurred in coding regions, resulting in frame shifted, have significant effects on the function of genes.

To identify the most important mutations related to inhibitor tolerance, common SNPs and InDels and their functions were displayed in **Fig.4**. It was then found that the common mutations occurred in the 7 evolved strains included 48 missense SNPs and 15

InDels resulting in frame shifted. It is interesting to note that among those 48 missense SNPs, 25 occurred at different positions of a gene, which is aligned to the one encoding reverse transcriptase (RHTO_02155) in *R. toruloides* NP11 (Zhu et al., 2012). However, there are no previous studies explaining the role of this gene in tolerance; so, the function of this mutant gene should be further identified. Another common missense mutation happened in a gene predicted as RHTO_01747 (coding for MFS transporter, quinate permease). Major facilitator superfamily (MFS) transporters are responsible for the bonding and transport of essential nutrients, ions and other compounds in a wide range of microorganisms (Rédei, 2008). A plasma membrane transporter belonging to the MFS family in *S. cerevisiae* was reported to show resistance to short-chain monocarboxylic acid and quinidine (Tenreiro et al., 2002). Deletion of genes encoding for MFS proteins was reported to promote a 3-fold reduction of coniferyl aldehyde in yeast (Sundström et al., 2010). The mutation of this gene may change the structure of membrane proteins, resulting in an improved tolerance of yeast to the inhibitors.

Among the 15 common InDels causing frame shifted, Δ1bp deletion was observed in RHTO_05744, a RIM9 protein encoding gene. RIM9 protein has been reported as relevant to a variety of responses to stress and to the yeast-hyphal transition (Yan et al., 2012). Another common Δ1bp deletion was found in RHTO_04597 (coding for ATP-binding cassette transporter, ABC), which contains a large family of proteins with a diversity of physiological functions (Bouige et al., 2005). Fungal ABC transporters have been reported to confer multiple drug resistance, stress response, cellular detoxification and resistance to weak organic acid (Wolfger et al., 2001;Prasad and Goffeau, 2012; Piper et al., 1998). In addition, ABC transporters play an important role to export toxic compounds and metabolites from intracellular environment, which is powered by TCA

408 processing (Liu, 2011). This could explain why the wild-type strain of *R. toruloides*
409 consumed all the carbon source during the cultivation but produced less lipids and
410 carotenoids than the evolved strains, as it probably used more energy to export
411 inhibitors from the intracellular environment. On the other hand, due to the improved
412 resistance to the inhibitors, evolved strains had more energy available for lipid and
413 carotenoid production.

414 Remarkably, two Δ1bp insertions were also found in different positions of an
415 oxidoreductase encoding gene domain (IPR000572) belonging to GO:0016491 in these
416 7 mutant strains. In this domain, xanthine dehydrogenase, aldehyde oxidase, nitrate
417 reductase and sulphite oxidase can be coded (Wootton et al., 1991). An evolved strain
418 of *S. cerevisiae* was found to have 1.92-fold higher vanillin reduction ability than the
419 wild-type strain due to up-regulated genes enriched in oxidoreductase activity
420 (GO:0016491) (Shen et al., 2014). Those frame shifted InDels may cause changes/loss
421 of gene functions; however, it was reported that disrupted multiple genes in *S.*
422 *cerevisiae* could result in higher tolerance and shorter lag phase in media containing
423 lactic acid (Suzuki et al., 2013). Although the mutations found in intergenic regions do
424 not change the amino acid sequence, it may still affect the gene splicing, transcription
425 factor binding, mRNA degradation and gene expression. In the present study, 149
426 common intergenic SNPs and 44 common intergenic InDel were found in the 7 evolved
427 strains of *R. toruloides*, which largely contributed to the genome variations of the
428 evolved strains. An investigation on stress-tolerance of *S. cerevisiae* demonstrated that
429 intergenic variants have significant impact on expression levels of stress tolerant genes,
430 resulting in stress resistant phenotypes of strains (Gan et al., 2018). To better understand
431 the impacts of intergenic mutations in *R. toruloides*, further studies should be done to

link the function of intergenic regions, relevant gene expression, and phenotype of strains. Finally, to obtain strains with better potential for industrial application, concentrated hydrolysates (containing higher concentration of sugars) should also be considered in subsequent ALE studies.

4. Conclusion

Adaptive laboratory evolution in hydrolysate-based medium was an effective strategy to obtain strains with improved ability to grow in medium containing biomass-derived inhibitory compounds. In fact, the adaptation strategy resulted in evolved strains of *R. toruloides* able to grow faster in hydrolysate containing inhibitory compounds, and also with better performance to accumulate lipids and carotenoids. Whole genome sequencing analysis allowed identifying common mutations in the evolved strains, giving useful indications on the mechanisms used by the strain to evolve. These findings are also relevant for the development of new strains with improved ability to convert biomass hydrolysates into valuable compounds.

Supplementary data

Supplementary figures and tables for this work can be found online.

Acknowledgement

This work was supported by the Novo Nordisk Foundation (NNF), Denmark (grant number NNF20SA0066233) and the China Scholarship Council (CSC), (grant number 201708530221).

456

457 **References**

458

459 1. Allen, S.A., Clark, W., McCaffery, J.M., Cai, Z., Lanctot, A., Slininger, P.J., Liu,
460 Z.L., Gorsich, S.W., 2010. Furfural induces reactive oxygen species accumulation
461 and cellular damage in Saccharomyces cerevisiae. Biotechnol. Biofuels 3, 1–10.
462 https://doi.org/10.1186/1754-6834-3-2
463 2. Arous, F., Frikha, F., Triantaphyllidou, I.-E., Aggelis, G., Nasri, M., Mechichi, T.,
464 2016. Potential utilization of agro-industrial wastewaters for lipid production by
465 the oleaginous yeast *Debaryomyces etchellsii*. J. Clean. Prod. 133, 899–909.
466 https://doi.org/10.1016/j.jclepro.2016.06.040
467 3. Avalos, J., Carmen Limón, M., 2015. Biological roles of fungal carotenoids. Curr.
468 Genet. 61, 309–324. https://doi.org/10.1007/s00294-014-0454-x
469 4. Ballesteros, L.F., Teixeira, J.A., Mussatto, S.I., 2014. Selection of the Solvent and
470 Extraction Conditions for Maximum Recovery of Antioxidant Phenolic
471 Compounds from Coffee Silverskin. Food Bioprocess Technol. 7, 1322–1332.
472 https://doi.org/10.1007/s11947-013-1115-7
473 5. Bonturi, N., Matsakas, L., Nilsson, R., Christakopoulos, P., Miranda, E.A., Berglund,
474 K.A., Rova, U., 2015. Single cell oil producing yeasts Lipomyces starkeyi and
475 Rhodosporidium toruloides: Selection of extraction strategies and biodiesel
476 property prediction. Energies 8, 5040–5052. https://doi.org/10.3390/en8065040
477 6. Bouige, P., Laurent, D., Piloyan, L., Dassa, E., 2005. Phylogenetic and Functional
478 Classification of ATP-Binding Cassette (ABC) Systems. Curr. Protein Pept. Sci. 3,
479 541–559. https://doi.org/10.2174/1389203023380486

7. Breuer, G., Evers, W.A.C., de Vree, J.H., Kleinegris, D.M.M., Martens, D.E., Wijffels, R.H., Lamers, P.P., 2013. Analysis of fatty acid content and composition in microalgae. J. Vis. Exp. 1–8. https://doi.org/10.3791/50628

8. Chandi, G.K., Gill, B.S., 2011. Production and characterization of microbial carotenoids as an alternative to synthetic colors: A review. Int. J. Food Prop. 14, 503–513. https://doi.org/10.1080/10942910903256956

9. Gan, Y., Lin, Y., Guo, Y., Qi, X., Wang, Q., 2018. Metabolic and genomic characterisation of stress-tolerant industrial Saccharomyces cerevisiae strains from TALENs-assisted multiplex editing. FEMS Yeast Res. 18, 1–13. https://doi.org/10.1093/femsyr/foy045

10. Ibraheem, O., Ndimba, B.K., 2013. Molecular adaptation mechanisms employed by ethanologenic bacteria in response to lignocellulose-derived inhibitory compounds. Int. J. Biol. Sci. 9, 598–612. https://doi.org/10.7150/ijbs.6091

11. Kitcha, S., Cheirsilp, B., 2013. Enhancing Lipid Production from Crude Glycerol by Newly Isolated Oleaginous Yeasts: Strain Selection, Process Optimization, and Fed-Batch Strategy. Bioenergy Res. 6, 300–310. https://doi.org/10.1007/s12155-012-9257-4

12. Liu, Z., Berg, C. Van Den, Weusthuis, R.A., Dragone, G., Mussatto, I., 2021. Strategies for an improved extraction and separation of lipids and carotenoids from oleaginous yeast. Sep. Purif. Technol. 257, 117946. https://doi.org/10.1016/j.seppur.2020.117946

13. Liu, Z., Feist, A.M., Dragone, G., Mussatto, S.I., 2020. Lipid and carotenoid production from wheat straw hydrolysates by different oleaginous yeasts. J. Clean. Prod. 249, 119308. https://doi.org/10.1016/j.jclepro.2019.119308

14. Liu, Z.L., 2011. Molecular mechanisms of yeast tolerance and in situ detoxification of lignocellulose hydrolysates. Appl. Microbiol. Biotechnol. 90, 809–825. https://doi.org/10.1007/s00253-011-3167-9

15. MarketsandMarkets, 2020. Carotenoids market worth $2.0 billion by 2026 [WWW Document]. Mark. Res. Rep.

16. Mussatto, S.I., Dragone, G.M., 2016. Biomass Pretreatment, Biorefineries, and Potential Products for a Bioeconomy Development, Biomass Fractionation Technologies for a Lignocellulosic Feedstock Based Biorefinery. Elsevier Inc. https://doi.org/10.1016/B978-0-12-802323-5.00001-3

17. Mussatto, S.I., Roberto, I.C., 2004. Alternatives for detoxification of diluted-acid lignocellulosic hydrolyzates for use in fermentative processes: a review. Bioresour. Technol. 93, 1–10. https://doi.org/10.1016/j.biortech.2003.10.005

18. Novoveská, L., Ross, M.E., Stanley, M.S., Pradelles, R., Wasiolek, V., Sassi, J., 2019. Microalgal Carotenoids : A Review of Production , Current Markets , Regulations , and Future Direction 1–21.

19. Piper, P., Mahé, Y., Thompson, S., Pandjaitan, R., Holyoak, C., Egner, R., Mühlbauer, M., Coote, P., Kuchler, K., 1998. The Pdr12 ABC transporter is required for the development of weak organic acid resistance in yeast. EMBO J. 17, 4257–4265. https://doi.org/10.1093/emboj/17.15.4257

20. Prasad, R., Goffeau, A., 2012. Yeast ATP-binding cassette transporters conferring multidrug resistance. Annu. Rev. Microbiol. 66, 39–63. https://doi.org/10.1146/annurev-micro-092611-150111

21. Probst, K. V., Schulte, L.R., Durrett, T.P., Rezac, M.E., Vadlani, P. V., 2016. Oleaginous yeast: a value-added platform for renewable oils. Crit. Rev. Biotechnol. 36, 942–955. https://doi.org/10.3109/07388551.2015.1064855

22. Ramos, M.J., Fernández, C.M., Casas, A., Rodríguez, L., Pérez, Á., 2009. Influence of fatty acid composition of raw materials on biodiesel properties. Bioresour. Technol. 100, 261–268. https://doi.org/10.1016/j.biortech.2008.06.039

23. Rédei, G.P., 2008. Major Facilitator Superfamily (MFS). Encycl. Genet. Genomics, Proteomics Informatics 62, 1142–1142. https://doi.org/10.1007/978-1-4020-6754-9_9778

24. Reyes, L.H., Gomez, J.M., Kao, K.C., 2014. Improving carotenoids production in yeast via adaptive laboratory evolution. Metab. Eng. 21, 26–33. https://doi.org/10.1016/J.YMBEN.2013.11.002

25. Shen, Y., Li, H., Wang, X., Zhang, X., Hou, J., Wang, L., Gao, N., Bao, X., 2014. High vanillin tolerance of an evolved Saccharomyces cerevisiae strain owing to its enhanced vanillin reduction and antioxidative capacity. J. Ind. Microbiol. Biotechnol. 41, 1637–1645. https://doi.org/10.1007/s10295-014-1515-3

26. Søltoft, M., Bysted, A., Madsen, K.H., Mark, A.B., Bügel, S.G., Nielsen, J., Knuthsen, P., 2011. Effects of organic and conventional growth systems on the content of carotenoids in carrot roots, and on intake and plasma status of carotenoids in humans. J. Sci. Food Agric. 91, 767–775. https://doi.org/10.1002/jsfa.4248

27. Sundström, L., Larsson, S., Jönsson, L.J., 2010. Identification of Saccharomyces cerevisiae genes involved in the resistance to phenolic fermentation inhibitors.

549 Appl. Biochem. Biotechnol. 161, 106–115. https://doi.org/10.1007/s12010-009-
550 8811-9
551 28. Suzuki, T., Sakamoto, T., Sugiyama, M., Ishida, N., Kambe, H., Obata, S., Kaneko,
552 Y., Takahashi, H., Harashima, S., 2013. Disruption of multiple genes whose
553 deletion causes lactic-acid resistance improves lactic-acid resistance and
554 productivity in Saccharomyces cerevisiae. J. Biosci. Bioeng. 115, 467–474.
555 https://doi.org/10.1016/j.jbiosc.2012.11.014
556 29. Tenreiro, S., Nunes, P.A., Viegas, C.A., Neves, M.S., Teixeira, M.C., Cabral, G.,
557 Sá-Correia, I., 2002. AQR1 gene (ORF YNL065w) encodes a plasma membrane
558 transporter of the major facilitator superfamily that confers resistance to short-
559 chain monocarboxylic acids and quinidine in saccharomyces cerevisiae. Biochem.
560 Biophys. Res. Commun. 292, 741–748. https://doi.org/10.1006/bbrc.2002.6703
561 30. Vasconcelos, B., Teixeira, J.C., Dragone, G., Teixeira, J.A., 2019. Oleaginous
562 yeasts for sustainable lipid production—from biodiesel to surf boards, a wide range
563 of “green” applications. Appl. Microbiol. Biotechnol.
564 https://doi.org/10.1007/s00253-019-09742-x
565 31. Wang, J., Gao, Q., Zhang, H., Bao, J., 2016. Inhibitor degradation and lipid
566 accumulation potentials of oleaginous yeast Trichosporon cutaneum using
567 lignocellulose feedstock. Bioresour. Technol. 218, 892–901.
568 https://doi.org/10.1016/j.biortech.2016.06.130
569 32. Wang, S., Sun, X., Yuan, Q., 2018. Strategies for enhancing microbial tolerance to
570 inhibitors for biofuel production: A review. Bioresour. Technol. 258, 302–309.
571 https://doi.org/10.1016/j.biortech.2018.03.064

572 33. Wolfger, H., Mamnun, Y.M., Kuchler, K., 2001. Fungal ABC proteins: Pleiotropic
573 drug resistance, stress response and cellular detoxification. Res. Microbiol. 152,
574 375–389. https://doi.org/10.1016/S0923-2508(01)01209-8
575 34. Wootton, J.C., Nicolson, R.E., Mark Cock, J., Walters, D.E., Burke, J.F., Doyle,
576 W.A., Bray, R.C., 1991. Enzymes depending on the pterin molybdenum cofactor:
577 sequence families, spectroscopic properties of molybdenum and possible cofactor-
578 binding domains. BBA - Bioenerg. 1057, 157–185. https://doi.org/10.1016/S0005-
579 2728(05)80100-8
580 35. Yan, L., Côte, P., Li, X.X., Jiang, Y.Y., Whiteway, M., 2012. PalI domain proteins
581 of Saccharomyces cerevisiae and Candida albicans. Microbiol. Res. 167, 422–432.
582 https://doi.org/10.1016/j.micres.2011.12.005
583 36. Zhu, Z., Zhang, S., Liu, H., Shen, H., Lin, X., Yang, F., Zhou, Y.J., Jin, G., Ye, M.,
584 Zou, H., Zhao, Z.K., 2012. A multi-omic map of the lipid-producing yeast
585 Rhodosporidium toruloides. Nat. Commun. 3, 1111–1112.
586 https://doi.org/10.1038/ncomms2112
587
588
589
590
591
592
593
594
595

596 **Figure captions**

597

598 **Fig. 1**. Growth profile of wild-type and evolved strains of *R. toruloides* cultivated in
599 non-decolorized (raw) wheat straw hydrolysate, non-supplemented (A) and
600 supplemented (B) with nitrogen source.

601

602 **Fig. 2**. Lipid and carotenoid accumulation by the wild-type and evolved strains of *R.*
603 *toruloides*. Carotenoid accumulation in mg/g cell and lipid accumulation in % (w/w).
604 Bars marked with two stars have a significant difference (p<0.05) compared with the
605 value of wild-type strain in each plot.

606

607 **Fig. 3**. Numbers and types of mutations identified in the 7 evolved strains of *R.*
608 *toruloides*. (A)SNPs and (B) InDels.

609

610 **Fig. 4**. Common mutations detected in the 7 evolved strains of *R. toruloides*.

611

612

613

614

615

616

617

618

619

Table 1. Composition of the wheat straw hydrolysates used for ALE experiments.

Compounds (g/L)	Non-decolorized (raw)	Decolorized
Glucose	40.88±0.54	39.27±0.27
Xylose	14.27±0.22	13.19±0.29
Acetic acid	1.54±0.03	1.49±0.13
Total phenolic compounds	1.51±0.04	0.53±0.00
Furfural	0.087±0.01	0.041±0.001
Levulinic acid	0.427±0.046	0.19±0.005
HMF	0.008±0.001	0.004±0.00
Vanillic acid	0.019±0.01	0.005±0.00
Syringic acid	0.016±0.004	0.003±0.00
4-hydroybenzaldehyde	0.037±0.002	0.012±0.00
Coumaric acid	0.056±0.01	0.003±0.00
Vanillin	0.022±0.004	0.002±0.00
Syringaldehyde	0.042±0.011	0.003±0.001

Table 2. Growth phenotypes of *R. toruloides* evolved in decolorized and non-decolorized wheat straw hydrolysates

Hydrolysates	Replicates	Number of passages	Initial concentration (%)	Final concentration (%)	Operation time
Decolorized hydrolysate	CH1	33	25	100	21 days
	CH2	28	25	100	
	CH3	29	25	100	
	CH4	35	25	100	
	CH5	25	25	100	
	CH6	27	25	100	
	CH7	27	25	100	
	CH8	27	25	100	
	CH9	27	25	100	
	CH10	23	25	100	
Non-decolorized (raw) hydrolysate	CH1	42	30	80	41 days
	CH2	46	70	100	
	CH3	34	10	60	
	CH4	42	70	100	
	CH5	43	80	100	
	CH6	41	80	100	
	CH7	42	80	100	
	CH8	43	80	100	
	CH9	41	80	100	
	CH10	38	80	100	

Table 3. Fatty acids produced by the wild-type (WT) and evolved (CH)strains of *R. toruloides* cultivated in non-decolorized hydrolysate supplemented with nitrogen source.

Strains	Fatty acids (mg/g of cells)						
	C14:0	C16:0	C16:1	C16:2	C18:0	C18:1	C18:2
WT	1.98±1.35	34.86±0.11	0.27±0.03	0.93±0.07	15.00±2.42	29.19±8.38	1.37±0.60
CH1	4.01±0.26	75.14±0.25	1.05±0.11	0.82±0.05	25.57±1.29	87.52±6.81	5.93±0.35
CH2	2.28±0.01	42.57±0.14	-	1.02±0.15	11.55±0.06	32.49±0.26	1.17±0.21
CH3	4.25±0.19	80.92±0.27	1.27±0.07	0.97±0.17	28.71±1.88	99.75±0.31	10.21±2.88
CH4	5.33±0.26	111.66±0.37	1.59±0.04	1.18±0.06	36.63±1.53	112.70±5.82	9.81±0.62
CH5	3.56±0.18	82.71±0.27	1.87±0.56	1.59±0.91	21.68±1.15	108.21±10.24	7.74±2.57
CH6	2.38±0.08	56.78±0.19	0.63±0.10	1.09±0.03	20.48±0.85	52.45±3.68	2.28±0.87
CH7	3.32±0.17	62.99±0.21	0.88±0.07	1.21±0.99	17.93±1.35	55.31±4.08	2.39±0.01
CH8	5.22±0.15	99.91±0.33	1.59±0.08	1.23±0.17	33.04±1.02	109.50±5.27	9.62±1.41
CH9	4.13±0.06	81.00±0.27	1.24±0.10	1.07±0.03	23.07±0.52	79.39±2.83	2.43±0.65
CH10	3.67±0.09	68.02±0.22	1.06±0.04	1.08±0.04	19.85±0.80	62.27±2.58	3.57±0.13

Table 4. Carotenoids produced by the wild-type (WT) and evolved (CH) strains of *R. toruloides* cultivated in non-decolorized hydrolysate supplemented with nitrogen source.

Strains	Carotenoids (mg/g of cells)		
	β-Carotene	γ-Carotene	Torulene
WT	0.57±0.01	4.09±0.45	3.20±0.27
CH1	0.56±0.00	4.75±0.0	4.07±0.02
CH2	0.98±0.00	6.33±0.06	6.58±0.03
CH3	0.56±0.00	5.48±0.22	4.59±0.18
CH4	0.55±0.00	5.70±0.09	4.30±0.13
CH5	0.78±0.00	5.33±0.18	5.82±0.50
CH6	0.57±0.01	6.33±0.18	5.18±0.10
CH7	0.98±0.11	5.99±0.03	7.13±0.09
CH8	0.60±0.00	5.38±0.02	4.04±0.40
CH9	0.86±0.00	6.12±0.04	6.67±0.20
CH10	0.86±0.00	6.07±0.09	6.34±0.07

620

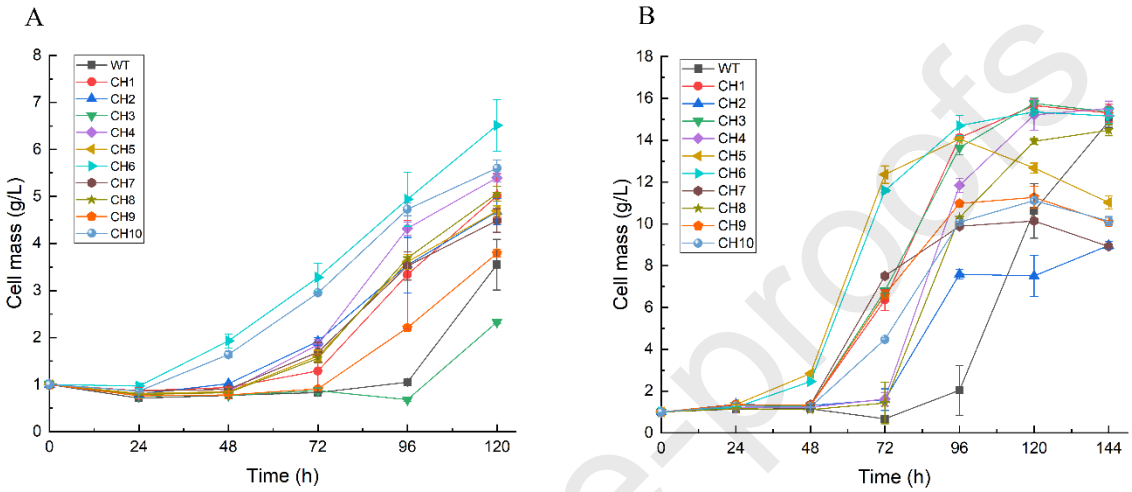

Figure 1

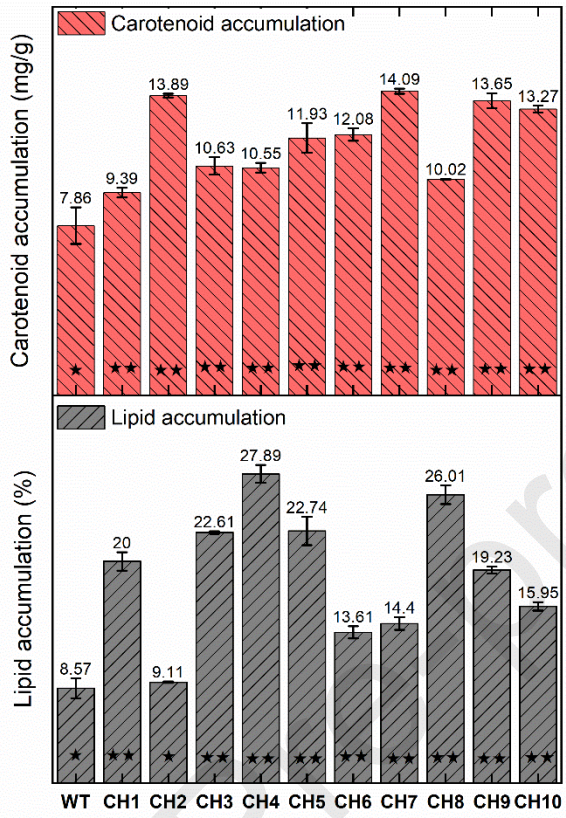

Figure 2

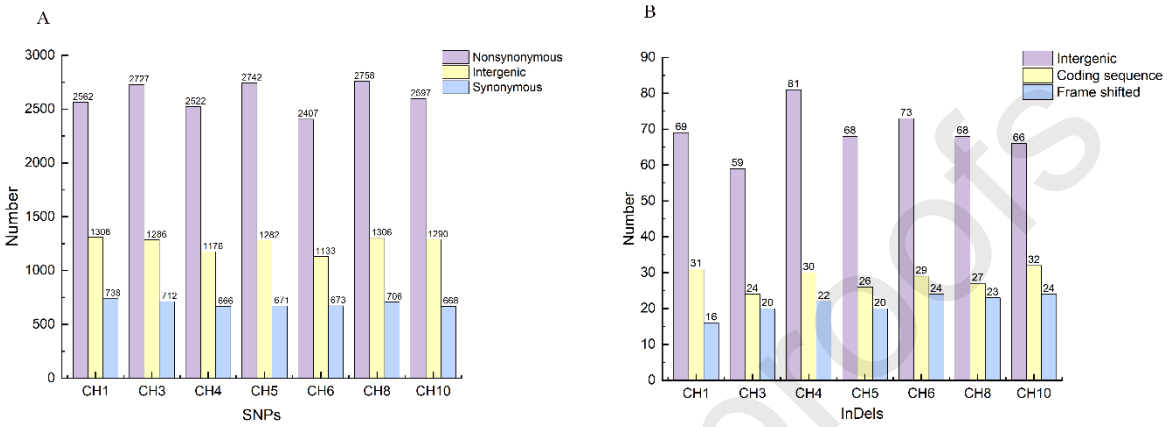

Figure 3

621

622

Number	Gene symbol	Function	Type	Base
B1	RHTO_05249	peptidyl-prolyl cis-trans isomerase, cyclophilin-type	Deletion	CAAGC
B2	RHTO_02556	secreted hydrolase	Insertion	C
B3	RHTO_05744	RIM9 protein	Deletion	A
B4	RHTO_01823	hypothetical protein	Deletion	CA
B5	RHTO_04597	ATP-binding cassette transporter	Deletion	G
B6	RHTO_04741	ATP-dependent rna helicase ded1	Insertion	TTGCTCGA
B7	RHTO_04972	Rho guanyl-nucleotide exchange factor	Insertion	AT
B8	RHTO_02328	glutamine-fructose-6-phosphate transaminase	Deletion	GC
B9	RHTO_06484	hypothetical protein	Deletion	A
B10	IPR000572	Oxidoreductase, molybdopterin-binding domain	Insertion	C
B11			Insertion	C
B12	RHTO_07799	exopolyphosphatase	Deletion	GGTCT
B13	RHTO_00039	hypothetical protein	Insertion	G
B14			Insertion	G
B15	RHTO_00040	solute carrier family 40 (iron-regulated transporter), member 1	Deletion	GG

Number	Gene symbol	Function	Codon change	Amino acid change
A1	RHTO_07574	hypothetical protein	AAC<->CAC	N<->H
A2	RHTO_01828	cyclin L1	AAC<->CAC	N<->H
A3	RHTO_01797	hypothetical protein	CAG<->CCG	Q<->P
A4			AGT<->CGT	S<->R
A5			ATG<->ACG	M<->T
A6	RHTO_01747	MFS transporter,quinate permease	TCT<->CCT	S<->P
A7	Sec16	COPII vesicle coat protein	GTT<->GGT	V<->G
A8	RHTO_07048	hypothetical protein	CAC<->CGC	H<->R
A9	RTG_01755	hypothetical protein	AGT<->TGT	S<->C
A10	Unknown	Unknown	AAC<->ACC	N<->T
A11	RHTO_00327	AP2-associated kinase	AGC<->GGC	S<->G
A12	RHTO_00514	phosphoribosyl-ATP pyrophosphohydrolase	TCC<->CCC	S<->P
A13	RHTO_06177	hypothetical protein	TTG<->GTG	L<->V
A14	RHTO_05528	zinc finger, SWIM-type domain containing protein	CTG<->CCG	L<->P
A15	RITO_02158	reverse transcriptase	GAG<->GGG	E<->G
A16	RHTO_05670	zinc finger, MYND-type domain containing protein	ATC<->ACC	I<->T
A17	RITO_06708	reverse transcriptase	ATG<->CTG	M<->L
A18	mst2	histone acetyltransferase mst2	CTG<->CAG	L<->Q
A19	RHTO_00030	tuberin	TCC<->CCC	S<->P
A20			AAG<->GAG	K<->E
A21			CAA<->CGA	Q<->R
A22			AAT<->GAT	N<->D
A23			AAT<->GAT	N<->D
A24			CCG<->CGG	P<->R
A25			TCC<->TTC	S<->F
A26			TCG<->TTG	S<->L
A27			CTT<->TTT	L<->F
A28			GAG<->GAC	E<->D
A29			GCC<->CCC	A<->P
A30			GGG<->AGG	G<->R
A31	RHTO_02155	reverse transcriptase	GTC<->ATC	V<->I
A32			CGA<->CAA	R<->Q
A33			GAG<->AAG	E<->K
A34			GGA<->AGA	G<->R
A35			GAC<->AAC	D<->N
A36			GAC<->AAC	D<->N
A37			GTC<->GAC	V<->D
A38			TTG<->TCG	L<->S
A39			TTG<->TCG	L<->S
A40			TCG<->CCG	S<->P
A41			TGG<->CGG	W<->R
A42			CTG<->CCG	L<->P
A43			TTG<->TCG	L<->S
A44			TCC<->GCC	S<->A
A45	RTG_03284	reverse transcriptase	GGA<->AGA	G<->R
A46	RHTO_07929	cytoplasm protein	AAG<->AGG	K<->R
A47	RTG_03284	reverse transcriptase	CGA<->CAA	R<->Q
A48	RHTO_07928	ribonuclease H	ACC<->AGC	T<->S

Figure 4

Highlights

625 A strategy of adaptive laboratory evolution in hydrolysate-based medium was
626 developed
627 Evolved strains of *Rhodosporidium toruloides* presented better tolerance to inhibitors
628 The strain's ability to accumulate lipids and produce carotenoids was also improved
629 Whole genome sequencing revealed tolerance-related genes in the wild-type strain